Calcium Coordination Studies of the Metastatic Mts1 Protein†

Kaushik Dutta,*,‡ Cathleen J. Cox,‡ He Huang, Ravi Basavappa, and Steven M. Pascal*

Department of Biochemistry and Biophysics, University of Rochester Medical Center, Box 712, Rochester, New York 14642

Received November 16, 2001

ABSTRACT: Mts1, also known as S100A4, is an 11 kDa calcium-binding protein strongly linked to metastasis. As a member of the S100 protein family, Mts1 is predicted to contain four α-helices and two calcium-binding loops, the second of which forms a canonical EF hand, while the first is a pseudo-EF hand, using two extra residues and principally backbone carbonyls rather than side chain oxygens to coordinate calcium. Here we follow chemical shift changes which occur in Mts1 upon titration of calcium. The results are consistent with calcium coordination by the EF hands described above. Filling of the first (pseudo) EF hand occurs at a lower calcium concentration than does filling of the second (canonical) EF hand. Concurrent with filling of site I, resonances from much of helix 4 vanish while the chemical shifts of a possibly nascent helical segment immediately C-terminal to helix 4 increase in helical character. Other smaller changes are seen, including a change in the linker joining helix 2 and helix 3. Since binding of effector molecules to S100 proteins has been shown to involve the C-terminus and linker regions, these calcium-induced changes have implications for the role of Mts1 in metastasis.

Metastasis is the process by which cells from a primary tumor break from the original mass and invade other tissues. Primary tumors are rarely fatal; more than 90% of fatalities result from secondary tumors. The Mts1 protein (also known as S100A4) has been linked to the metastatic process in several ways. First identified via its upregulation in rat mammary epithelial cells with mutated morphology (*1*), Mts1 has since been shown to be expressed to detectable levels in metastatic but not nonmetastatic tumors (*2*−*5*), and its introduction into nonmetastatic cell lines confers a metastatic phenotype (*6*−*10*). Cross-breeding of Mts1 transgenic mice with tumor-prone mice produces offspring with increased tumor aggressiveness (*11*), and antisense ribozyme targeting of Mts1 reduces the metastatic character of tumor cells (*6*, *12*, *13*). The ability of Mts1 to bind the heavy chain of nonmuscle myosin II in a calcium-dependent manner (*14*−*16*) and to partially depolymerize myosin filaments (*14*, *17*), together with the cell morphology changes mentioned above, has led to the suggestion that Mts1 induces metastasis through disruption of the cytoskeleton.

Mts1 belongs to the S100 protein family (for a review, see ref *18*), members of which have been implicated in a wide variety of cellular functions, including inflammation, cytoskeletal dynamics, cell growth and differentiation, and calcium homeostasis. Atomic resolution structures of several S100 proteins have been determined (see Figure 1), revealing the presence of dimerization in most cases. Each monomer unit contains four helices, and dimerization takes place principally through an antiparallel alignment of helix 1 with helix 1′ and helix 4 with helix 4′, where the primes distinguish monomer units. In most cases, calcium-binding loops are present between helix 1 and helix 2, and also between helix 3 and helix 4, allowing two calcium atoms to bind per monomer. The second calcium-binding loop is a canonical EF hand, using principally side chain oxygen atoms over a 12-residue stretch to coordinate the calcium cation. The first loop is a so-called pseudo-EF hand, using principally backbone carbonyls over a 14-residue stretch to coordinate the cation. Calcium-induced conformational changes have been detected, and linked to the ability of several S100 proteins to interact with effector molecules (*19*−*23*). The most highly conserved sequences of S100 proteins are the EF hands, while the regions between helix 2 and helix 3 (linker) and the N- and C-termini are the least conserved. These more variable regions, especially the C-terminus and linker, along with portions of the helices, have been implicated in the interactions described above.

Here we have used primarily NMR[1] spectroscopy to examine the effect of calcium titration upon murine Mts1. Results are consistent with a considerable change in the conformation of the calcium-binding loops and with conservation of three of the four helices. However, most of helix 4 becomes unobservable, while the chemical shifts of the region immediately C-terminal to helix 4 become increasingly helical in character at higher calcium concentrations. NMR data reveal calcium-binding affinities in the micromolar range or lower for each of the EF hands, with somewhat higher affinity for EF hand I. Interestingly, the changes in helix 4 and the C-terminus, a region likely to be important for interaction with myosin, appear to occur in conjunction with filling of EF hand I. However, other data suggest that filling of both EF hands may be necessary for the myosin interaction.

† R.B. is a Research Scholar of the Leukemia and Lymphoma Society of America.

* To whom correspondence should be addressed. Phone: (716) 273-4832. Fax: (716) 275-6007. E-mail: pascal@oxbow.biophysics.rochester.edu or kaushik_dutta@urmc.rochester.edu.

‡ These authors contributed equally to this work.

[1] Abbreviations: NMR, nuclear magnetic resonance; HSQC, heteronuclear single-quantum coherence; CSI, chemical shift indexing.

10.1021/bi012061v CCC: $22.00
Published on Web 03/06/2002

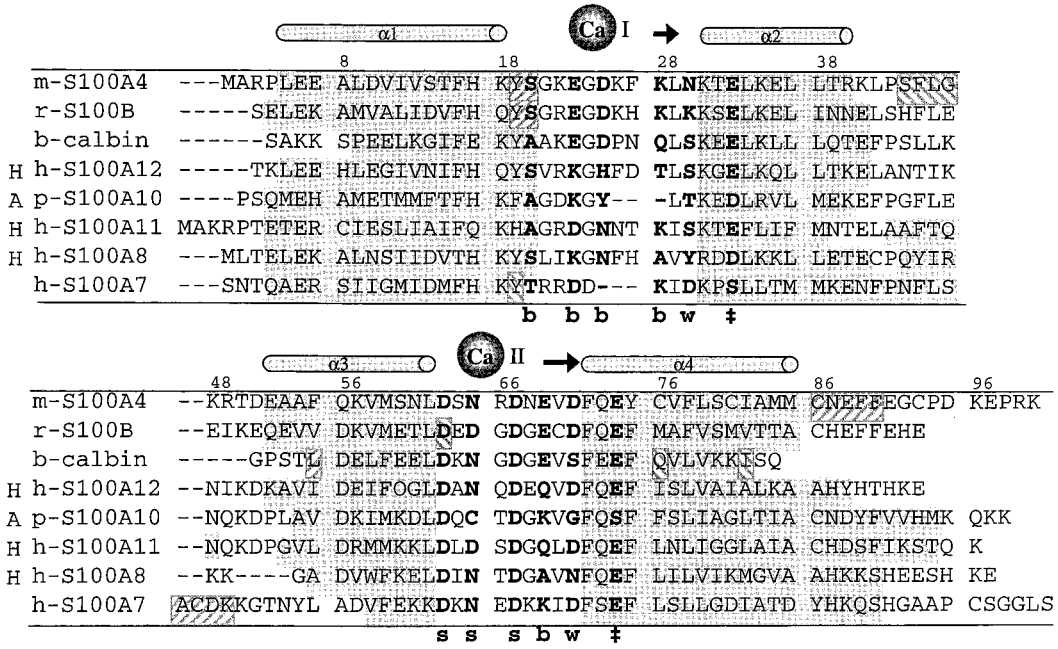

FIGURE 1: Sequence alignment of selected S100 proteins. The sequential numbering along the top refers to the Mts1 (S100A4) sequence. The calcium-coordinating residues of the pseudo-EF and canonical EF hands (residues 20−33 and 63−74 in Mts1, respectively) are in bold, and are labeled below the S100A7 sequence according to whether they coordinate calcium via a backbone carbonyl oxygen (**b**), one side chain oxygen (**s**), two side chain oxygens (**‡**), or a bridging water molecule (**w**). The extent of helices 1−4 is shown via shading. S100A10 helices are from the structure of the apo form, and S100A8, -A11, and -A12 are from the holo form. For the other proteins, the helical extent is shown for both forms, with backward and forward leaning diagonal shading representing helical regions present in only the apo and holo forms, respectively. The arrows denote β-like stretches in apo and holo Mts1. References: apo (*25*) and holo (this study) murine S100A4, apo (*35*) and holo (*34*) racine S100β, apo (*36*) and holo (*37*) bovine calbindin$_{9k}$, holo human S100A12 (*38*), apo porcine S100A10 from a complex with an annexin II peptide (*22*), holo human S100A11 from a complex with an annexin I peptide (*39*), holo human S100A8 (*40*), and apo (*41*) and holo (*42*) human S100A7.

MATERIALS AND METHODS

NMR Sample Preparation. Murine Mts1 was expressed using the H-MBP-3C vector system (*24*) and purified as described previously (*25*). The apo NMR sample was prepared by concentrating purified Mts1 to 1.3 mM in 5 mM Tris-HCl and 1 mM EDTA at pH 6.0. This sample was brought to 5% D_2O and 50 μM NaN_3. The protein concentration was estimated via absorbance at 280 nm using the theoretical ϵ_{280} of 2800.

NMR Spectra. All NMR experiments were performed on a Varian INOVA 600 MHz NMR spectrometer at 40 °C. $^1H-^{15}N$ heteronuclear single-quantum coherence (HSQC) spectra were recorded using a sensitivity-enhanced gradient pulse scheme (*26*). A total of eight transients were accumulated with a recycle delay of 1 s for each of the 128 complex increments for all titration points except for the last (7.6 equiv) for which 32 transients were acquired. The ^1H and ^{15}N sweep widths were 8000 and 2400 Hz, respectively. Data processing was carried out with nmrPipe (*27*), and spectra were analyzed with NMRview (*28*). Resonance assignments of apo Mts1 have been described previously (*25*), and complete holo assignments will be reported elsewhere.

Calcium Titration. Four stock solutions containing 25 mM, 50 mM, 100 mM, and 1 M $CaCl_2$ were prepared, in 5 mM Tris-HCl at pH 6.0. These buffers were treated with Chelex 100 before addition of calcium to remove trace amounts of metal. Two-dimensional (2D) $^1H-^{15}N$ HSQC spectra were recorded at each titration step. All $CaCl_2$ aliquots were added directly to the NMR sample, and the resealed NMR tube was briefly vortexed. The first five titration points were performed by adding 0.2 equiv of calcium from the 50 mM $CaCl_2$ stock solution and the next five by adding 0.4, 0.3, 0.3, 0.3, and 0.5 equiv from the 25 mM stock, followed by 0.9 and 4.3 equiv from the 100 mM and 1 M $CaCl_2$ stock solutions, respectively. The amount of calcium needed to saturate the EDTA was estimated by the point at which HSQC peaks begin to migrate noticeably. There was negligible change in pH after addition of $CaCl_2$. The total volume increase was 37 μL, and the change in protein concentration due to dilution was incorporated into the data analysis. By following the movement of HSQC peaks between each titration point, the assignment of backbone $HN-^{15}N$ cross-peaks at intermediate concentrations of calcium was accomplished. Chemical shifts of resonances which could not be detected at several intermediate calcium concentrations were interpolated as a linear function of equivalents of calcium added.

RESULTS AND DISCUSSION

Figure 2 shows the $^1H-^{15}N$ HSQC spectra of apo (black) and holo or calcium-loaded (red) Mts1. The dashed lines connect apo and holo resonances of selected residues whose chemical shifts are altered substantially upon calcium titration. Blue dashed lines denote residues from EF hand I and green dashed lines those from EF hand II, and residue 88 (black dashed line) is C-terminal to helix 4. A more quantitative indication of chemical shift change is shown in Figure 3, which contains plots of the square root of the sum of the squares of changes in backbone HN and ^{15}N chemical shifts of each residue as the calcium concentration is

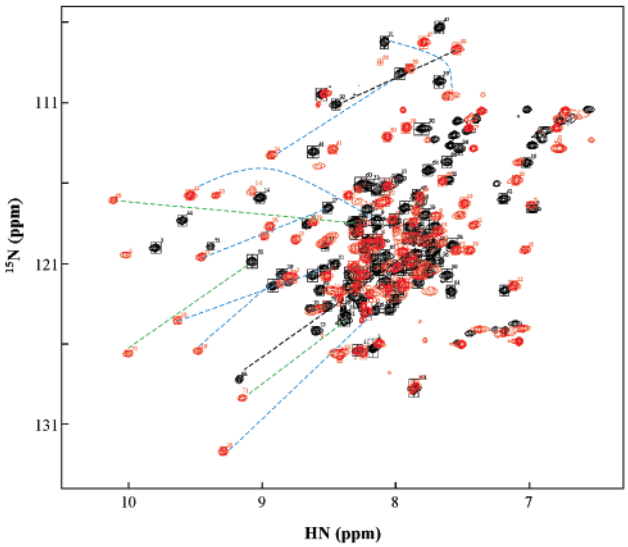

FIGURE 2: Superposition of ^{1}H−^{15}N HSQC spectra of apo (black) and calcium-loaded (red) Mts1. Apo and holo peaks from selected residues are connected by dashed lines: blue for residues from EF hand I, green for EF hand II, and black for E88 from the C-terminus.

increased incrementally. Figure 3a shows the difference between the chemical shifts at each increment and the apo chemical shifts ($\Delta\delta$). The chemical shifts of the two EF hands change substantially over the course of the titration (Figure 3a, top panel), while those from the first three helices change minimally, with the exception of the N-terminus of helix 2 which is part of EF hand I (see Figure 1). The fourth helix becomes broadened, and we were not able to assign most of its resonances in the holo state (residues 13, 19, 44, 45, and 76−86 are not assigned in the holo state, whereas all apo backbone HN and ^{15}N resonances were assigned). This would suggest that dynamic processes are present at or near helix 4, causing a change in environment on a millisecond to microsecond time scale. These processes may or may not be related to calcium exchange. The changes in chemical shifts of the C-terminal residues just past helix 4 are similar in magnitude to the changes in the EF hands.

Figure 3b shows the difference between chemical shifts in sequential increments [$\Delta(\Delta\delta)$], which can give a clearer picture of the order of changes with respect to the progression of the titration. Large chemical shift changes in EF hand I begin to occur at 0.2 equiv of calcium and are nearly complete by the 1.0 equiv level. Substantial changes in EF hand II chemical shifts begin to occur near the 0.6−1.0 equiv level, and continue until close to 2.0 equiv is added. Taken together, these data indicate that calcium first titrates into site I and thus that EF hand I has a higher affinity for calcium than EF hand II. This also suggests that binding of the two

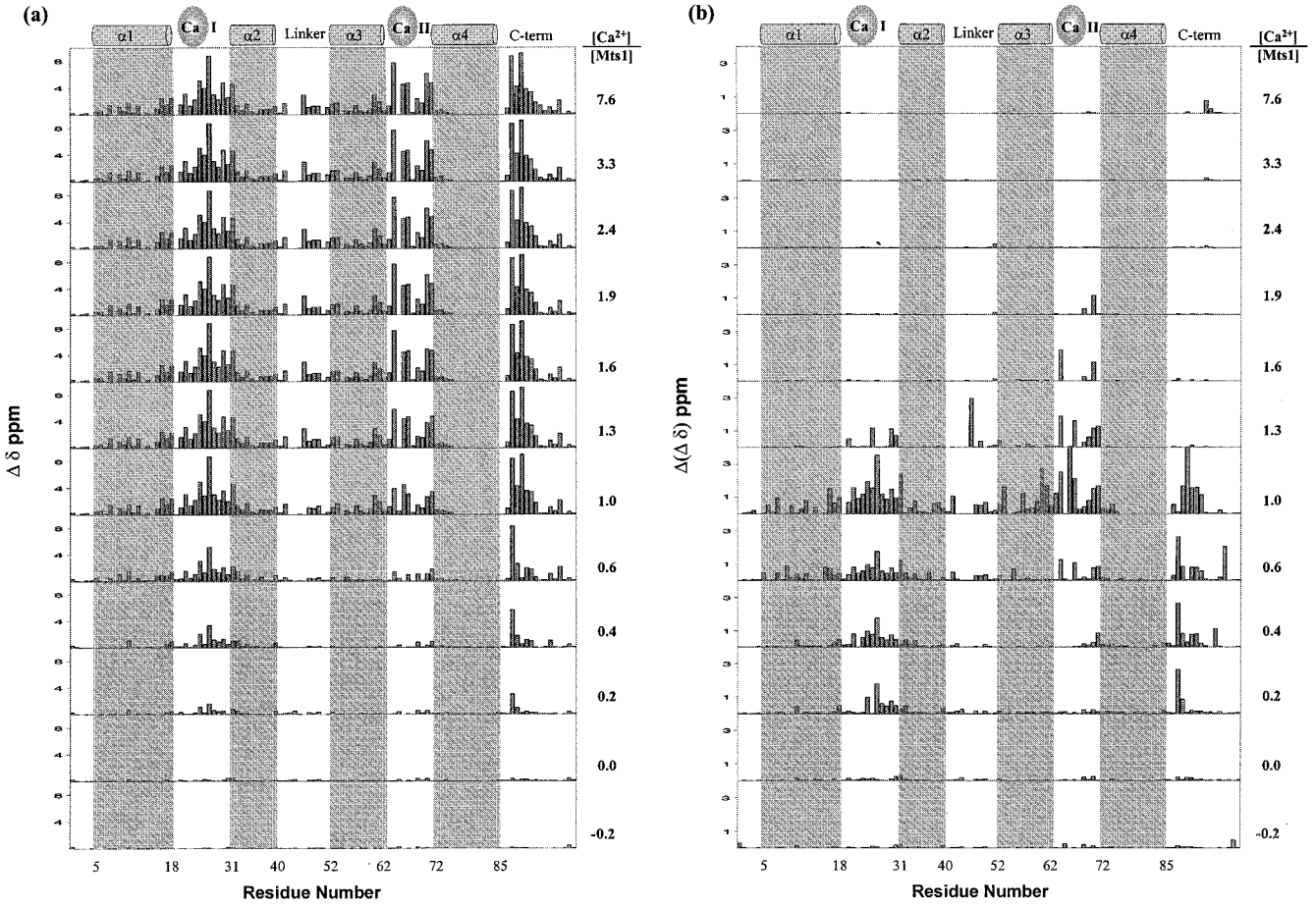

FIGURE 3: Change in chemical shifts of ^{15}N−^{1}H HSQC backbone cross-peaks as a function of calcium concentration. Secondary structural elements are shown along the top, and calcium equivalents are shown to the right. (a) Difference between chemical shifts at the specified equivalent level and the apo chemical shifts. $\Delta\delta$ values are the square root of the sum of the squares of changes in backbone HN and ^{15}N chemical shifts of each residue. (b) Difference between chemical shifts at the specified equivalent level and those of the preceding titration point [$\Delta(\Delta\delta)$]. Note that residues 13, 19, 44, 45, and 76−86 were not assigned in the holo state or for titration steps at approximately ≥1.0 equiv, and thus, data for these residues are omitted at higher equivalent levels.

Table 1: Backbone ^{15}N Chemical Shifts of Residues Adjacent to Calcium-Coordinating Backbone Carbonyls

protein	EF hand	position	residue	δ (apo)	$\Delta\delta$ (halo − apo)	$\Delta\delta^a$ (1 equiv − apo)	$\Delta\delta^a$ (holo − 1 equiv)
S100β^b	1	2	G19	107.28	2.89		
	1	5	G22	109.13	–		
	1	7	K24	126.12	–		
	1	10	L27	120.24	5.39		
	2	8	C68	120.08	4.88		
calbindin$_{9k}^b$	1	2	A15	114.19	2.58	−0.043	4.44
	1	5	G18	108.21	4.66	1.02	0.49
	1	7	P20	–	–	–	–
	1	10	L23	120.33	4.00	−0.06	4.06
	2	8	V61	118.22	8.03	8.07	0.24
Mts1	1	2	G21	107.53	3.07	3.04	0.03
	1	5	G24	109.30	5.00	4.91	0.09
	1	7	K26	124.02	8.66	8.61	0.05
	1	10	L29	121.78	4.71	3.54^c	1.17^c
	2	8	V70	120.62	6.04	2.60^c	3.44^c

^{a} Data for analysis (1 equiv) of calbindin$_{9k}$ obtained from titration of cadmium instead of calcium. ^{b} All data for S100b and calbindin$_{9k}$ from Feeney and co-workers (*29*). ^{c} Chemical shifts at 1 equiv for these residues are interpolated as described in the text.

calcium ions is not strongly cooperative. Changes in the C-terminus appear to roughly mirror the changes in EF hand I, beginning at 0.2 equiv and ending by 1.0 equiv. Most helix 4 resonances begin to reduce in intensity at the 0.2 equiv level, and vanish by 0.6 equiv, also suggesting a relation to the titration of the first calcium. However, additional changes to residues with unobservable peaks during titration of the second calcium cannot be ruled out. Changes in the linker region between helix 2 and helix 3 appear to occur mostly during titration of the first calcium, although an abrupt change is seen at 1.3 equiv in the chemical shift of L46, which is discussed further below.

Feeney and co-workers (*29*) performed a comparison study of EF hand proteins which included analysis of the change in backbone ^{15}N chemical shifts of two S100 proteins, S100β and calbindin$_{9k}$. One conclusion was that the ^{15}N resonances of residues immediately following backbone carbonyl carbons which directly coordinate calcium move downfield in a significant and predictable manner. Table 1 shows results for S100β and calbindin$_{9k}$, along with a similar analysis for Mts1. Since four backbone carbonyls coordinate calcium in EF hand I, and one is used by EF hand II (see the legend of Figure 1), analyses of five residues are presented in the table. The values of the apo chemical shifts (column 5) and their changes upon complete calcium titration (column 6) are consistent from protein to protein, although not all resonances could be assigned in S100β and calbindin$_{9k}$. The average change in these five residues (those that could be measured) is 4.39, 4.82, and 5.50 ppm for S100β, calbindin$_{9k}$, and Mts1, respectively, with the increased average for Mts1 resulting from the large shift of K26 (8.66 ppm), the analogue of which was not assigned in the other two proteins.

Through examination of the amount of change which occurs during titration of the first and second equivalent separately, disparities arise between calbindin$_{9k}$ and Mts1. The affinities of the two EF hands in calbindin$_{9k}$ are reportedly very similar, and furthermore, calcium binding is cooperative, with filling of the second site being more favorable once the first site is filled (*29*). For this reason, to examine calbindin$_{9k}$ with only one site filled, cadmium has been used in place of calcium (*30*, *31*). The rationale is that a change in ion size and characteristics can be more easily accommodated by site II, which employs side chains for coordination, than by site I, which employs backbone atoms.

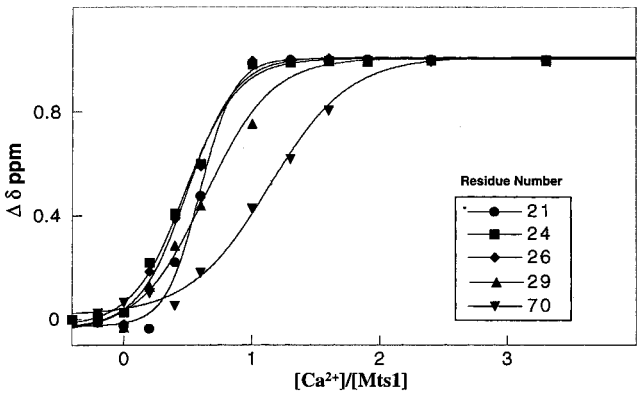

FIGURE 4: Chemical shift titration curves for the ^{15}N−^{1}H HSQC backbone peaks immediately adjacent to the five backbone carbonyl oxygens which coordinate calcium. Note that V70 titrates at a higher calcium concentration than those from site I.

Thus, the affinity of site I is decreased sufficiently to separate filling of the sites. At the level of 1.0 equiv of cadmium, the calbindin$_{9k}$ EF hand I resonances have shifted by an average of 0.18 ppm, while the EF hand II resonance has shifted by 8.07 ppm (*29*). During titration of the second equivalent, site I resonances shift an average of 3.00 ppm, while the site II peak moves 0.24 ppm. In contrast, the fillings of the two Mts1 sites are separated even when using calcium. The G21, G24, and K26 resonances from Mts1 site I shift an average of 5.52 ppm during titration of the first equivalent, and 0.06 ppm during the second. The L29 and V70 peaks are not observable at 1.0 equiv presumably because of exchange broadening. However, by interpolation as described in Materials and Methods, the L29 resonance apparently shifts primarily during the first equivalent, and V70 mostly during the second. These points are illustrated graphically in Figure 4. These results appear to confirm that calcium coordination occurs by a mechanism in Mts1 similar to that in other S100 proteins, utilizing the residues denoted in Figure 1 (bold letters), but that filling of the calcium-binding loops is somewhat sequential in character, and is reversed in order as compared to cadmium filling of calbindin$_{9k}$ sites. The fact that titration appears to be complete near 2.0 equiv suggests that both calcium sites have K_d values in the micromolar range or lower (NMR samples are ~1.3 mM in Mts1). These results corroborate data from Dukhanina and co-workers (*32*), who previously have reported a higher

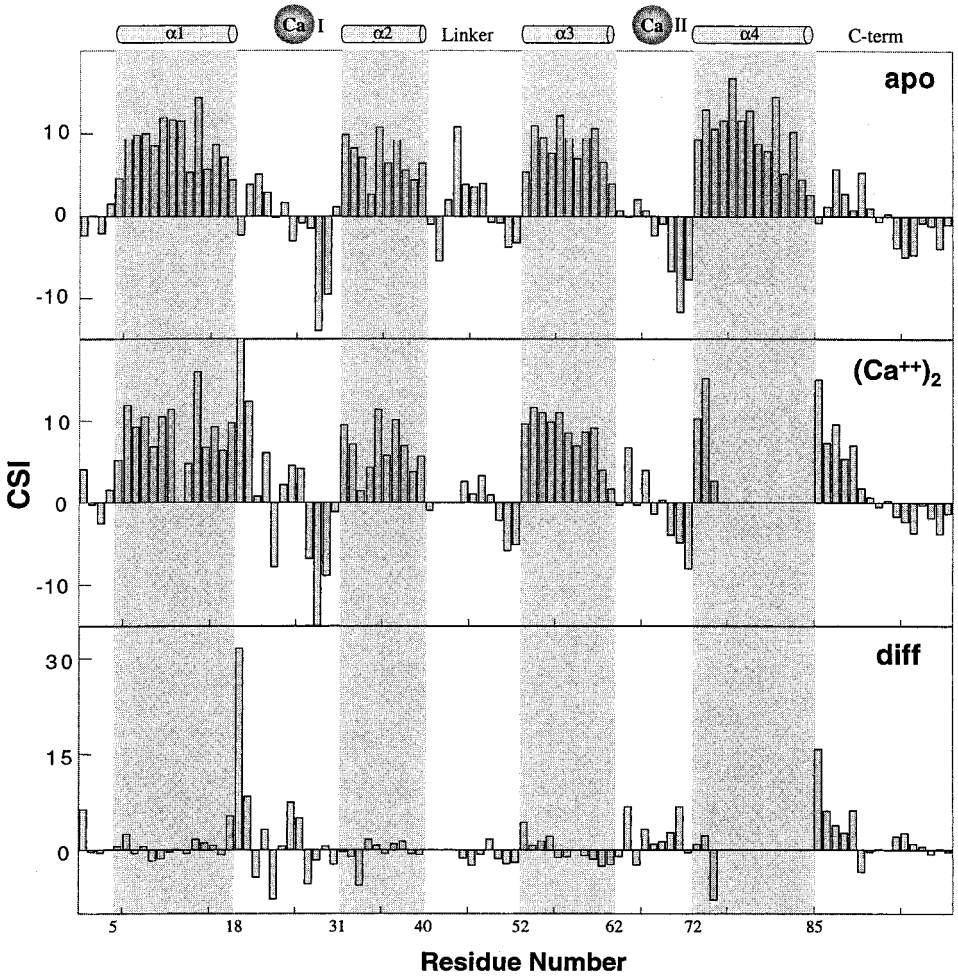

FIGURE 5: CSI values for apo (top) and calcium-loaded (center) Mts1 and their difference [CSI(Ca^{2+})$_2$ − CSI(apo)] (bottom). The secondary structure is labeled along the top. Data for the holo state were not available for the residues listed in the legend of Figure 3, and therefore, differences were not calculated for these residues.

calcium affinity of site I versus site II in Mts1 using other methods, and suggest that Mts1 in the presence of approximately 1 equiv of calcium may be useful as a model system in which site I is largely filled and site II is principally vacant.

Comparison of the sequences of Mts1 and calbindin$_{9k}$ (Figure 1) offers no obvious explanation for the differences in filling characteristics of the sites in the two proteins. First, it should be noted that alterations of the calbindin$_{9k}$ sequence which either increase the affinity of site I, decrease the affinity of site II, or decrease cooperativity could contribute to the observed results. With this in mind, it is interesting to note that three of the 12 residues which directly or indirectly (through water) coordinate calcium (Figure 1) differ between the two proteins. These are Q25 and S27 from site I and S65 from site II of calbindin$_{9k}$, which are replaced by K28, N30, and D71 in Mts1, respectively. Thus, the Mts1 site I ligands gain a positive charge and site II ligands a negative charge, with respect to calbindin$_{9k}$. Both of these modifications would appear to be in contradiction to the observed changes in filling order by positively charged calcium ions. In total, the 14 residues of site I in calbindin$_{9k}$ and Mts1 have charges of -2 and $+1$, respectively, while the 12 residues of site II carry a charge of -4 in each case. Since the second site coordinates calcium principally via side chain contacts, it is not surprising that site II side chains carry more negative charge, but again the charge difference between site I of calbindin$_{9k}$ and site I of Mts1 would seem to be at odds with the observed filling order. Total charge cannot be the only factor, a point which is further supported by the fact that cooperative binding of calcium in calbindin$_{9k}$ clearly would not occur if only total charge were considered. The geometry of coordination must also be important. Other substitutions which may contribute to the observed effect include site II residues G60 and E67 in calbinin$_{9k}$, which are replaced by R66 and Q73 in Mts1, respectively, and site I residues P23 and N24 in calbindin$_{9k}$, which are replaced by K26 and F27 in Mts1, respectively. There are also changes in the sequence of the short β-like stretches (see below), which are involved in interaction between the two EF hands in several S100 proteins. Changes here could potentially affect cooperativity as well as individual affinities.

As mentioned, many of the HSQC resonances become unobservable during the titration, particularly near the point of 1.0 equiv of calcium, and reappear again at higher calcium concentrations. This is evidence of intermediate exchange, which occurs when the time scale of a dynamic process is similar to the difference in chemical shift ($\Delta\delta$) between the two conformers (assuming only two conformers for this discussion). Broadening to baseline of several calcium loop peaks with $\Delta\delta$ values of $\sim$500 Hz suggests that calcium may exchange from the binding sites on a high microsecond to low millisecond time scale. On the other hand, several residues near the N- and C-termini and in the linker produce

two broadened peaks near the level of 1.0 equiv of calcium. Since the chemical shift changes of the doubled residues are in the 50 Hz range, this suggests slower (high millisecond) dynamics. Much of this doubling and associated broadening survives in the case of the calcium-saturated state. These facts appear to indicate that the calcium-loaded conformation possesses high millisecond dynamics near the termini and linker, which also influences the spectra at intermediate titration points. The previously discussed inability to observe helix 4 resonances in the calcium-loaded state may be related to this slower motion. Note that the termini and linker regions of other S100 proteins have been shown in a number of cases to interact with effector molecules (*19*−*23*).

Using C_α, C_β, and backbone C-carbonyl chemical shifts, chemical shift indexing [CSI (*33*)] of the apo and holo forms was performed (Figure 5) to detect secondary structural elements. As reported previously (*25*), four principal helices are detected in the apo form (Figure 5, top). These helical residues are shaded in Figure 1, along with the helical regions of other S100 proteins. Short helical stretches also appear to be present in apo Mts1 residues 20−22 and 44−47, with short β-like stretches within each EF hand immediately preceding helix 2 and helix 4, at residues 28 and 29 and 69−71, respectively.

The principal points of secondary structure variability in S100 proteins are the linker region and the C-terminus. The linker region of apo Mts1 appears to contain approximately one turn of helix (residues 44−47), which is seen in three of the other seven S100 proteins in Figure 1. In S100A7, this helical stretch apparently is an extension of helix 2. Helix 4 of several S100 proteins can be extended by as many as nine residues further than in Mts1. Note though that S100β helix 4 is of the same length as that of Mts1, and S100A12 is only two residues longer. Also note that Mts1 appears to possess some helical character in residues 87−92. This could be indicative of nascent or transient helical character in this region, which may form a short fifth helix or may extend helix 4.

In the calcium-loaded form, four principal helices are again seen (Figure 5, center) with some alterations. Helix 1 appears to lengthen by two residues, similar to the occurrence in S100β. This brings the helical terminus to a conserved position relative to the other S100 proteins. The helical stretch of residues 44−47 may be somewhat destabilized, whereas the helicity of the linker region in most S100 proteins does not appear to be strongly affected by calcium titration. The most notable changes in Mts1 conformation are in helix 4 and the associated C-terminus. Most of helix 4 becomes unobservable as noted above, and the chemical shifts of the C-terminus become more helical in character. Whether the bulk of helix 4 actually remains intact cannot be ascertained from the NMR spectra, but circular dichroism spectroscopy indicates that the percentage helical content does not change substantially, and if anything increases, upon calcium titration (data not shown). Interruptions in the unobservable portion of helix 4 upon titration, as occurs in calbindin$_{9k}$, cannot be ruled out. However, it appears that the C-terminal end of helix 4 extends in the holo form to a point similar to that of helix 4 from S100A7 and -A8, although as mentioned above there is some evidence of helicity in this region also in the apo form.

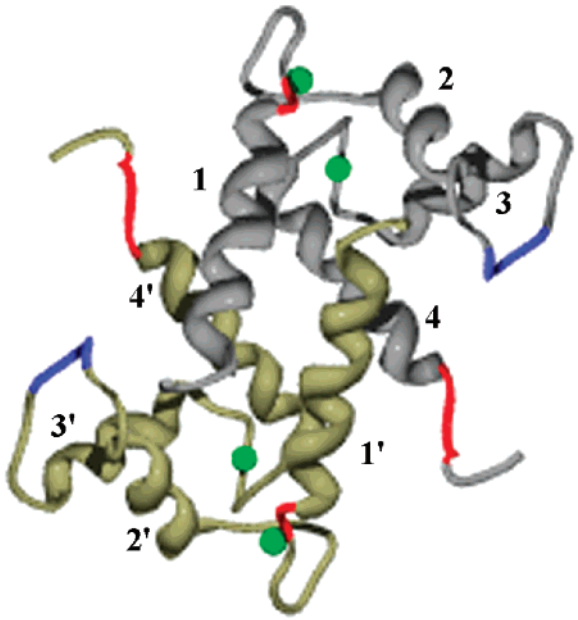

FIGURE 6: Model of Mts1 based upon the holo S100β coordinates (*34*). The four helices of the first monomer unit are silver and are labeled 1−4, while those of the second monomer are gold and are labeled 1′−4′. The regions with increased CSI values (increased helical character) upon calcium titration are shown in red. These are residues 19 and 20 following helix 1 and helix 1′ and residues 86−90 following helix 4 and helix 4′. The portion of the linker region which decreases in helical character upon titration is shown in blue. Calcium ions are green. Rendering was performed with SWISS-MODEL and Swiss-PdbViewer (*43*) and postprocessed with POV.

The changes in the secondary structure of the C-terminus and helix 4 appear to be linked to titration of the first calcium into site I, while the loss of helical character in residues 44−47 is partially associated with filling of each calcium site. HSQC peaks for residues 47−49 vanish after 0.4 equiv and reappear at 1.0 or 1.3 equiv, while those of S44 and F45 vanish after 0.6 and 0.2 equiv, respectively, and could not be assigned with a higher number of equivalents. The apo L46 peak remains relatively stationary throughout, but a second shifted L46 peak arises abruptly at 1.3 equiv and remains. Extension of helix 1 is related to filling of site I.

Figure 6 shows a homology model of Mts1 based on the structure of calcium-loaded S100β (*34*). In red are regions with altered CSI values indicating helix formation upon titration of the first calcium, namely, extension of helix 1 and helix 4. In blue is part of the linker region which loses helical character in conjunction with filling of both calcium sites. The pattern by which these changes ring the circumference of the structure is striking. The change in helix 1 is directly related to titration of the calcium to the adjacent site I, but the changes in the linker and the C-terminus (extension of helix 4) would appear to require transmission of information over a longer distance. The disappearance of helix 4 peaks suggests the intriguing possibility that helix 4 may shift in position or conformation sufficiently to bring the C-terminus into position to interact with another part of the protein, possibly helix 1′ or helix 2.

The calcium-induced changes in Mts1 described here have implications for the calcium-dependent interaction between Mts1 and myosin (*14*−*16*). In several cases, S100 proteins have been shown to interact with effector proteins using the linker region between helix 2 and helix 3 [e.g., S100β with

p53 (*20*) and S100A10 with annexin II (*22*)] or helix 4 and the associated C-terminus [S100β with p53 (*20*), with CapZ (*19*, *23*), and with other S100 proteins in an interaction apparently unrelated to typical heterodimerization (*21*)]. In Mts1, the association of both the vanishing of helix 4 resonances and formation/stabilization of the helix 4 extension with titration of the first calcium (site I) seems to suggest that if myosin binds to the C-terminus, the Mts1−myosin interaction may be possible in the presence of lower levels of calcium insufficient to fill site II. On the other hand, if the linker is involved, the myosin interaction may require changes which occur during titration of the second equivalent. Possible unobservable changes in helix 4 position, conformation, or dynamics during titration of the second equivalent may also be required.

In conclusion, observation of chemical shift values has been used to examine conformational changes in Mts1 upon calcium titration. Both putative EF hands bind calcium with sub-millimolar affinity, with site I filling earlier than site II. Changes in the region immediately C-terminal to helix 4 and the disappearance of many helix 4 resonances suggest that helix 4 may become extended and participate in a dynamic equilibrium, and the timing of these changes suggests that they may be closely associated with titration of the first calcium into site I. Changes occurring in site II and other possible changes in helix 4 are associated with filling of the second calcium site, while changes in the linker are associated with filling of both sites. These alterations are likely to be factors contributing to the calcium-dependent nature of the Mts1−myosin interaction as part of the process by which Mts1 induces metastasis.

ACKNOWLEDGMENT

We thank Hironao Wakabayashi, Andrei Alexandrov, and Scott Kennedy.

REFERENCES

1. Barraclough, R., Dawson, K. J., and Rudland, P. S. (1982) *Eur. J. Biochem. 129*, 335−341.
2. Ilg, E. C., Schafer, B. W., and Heizmann, C. W. (1996) *Int. J. Cancer 68*, 325−332.
3. Pedrocchi, M., Schafer, B. W., Mueller, H., Eppenberger, U., and Heizmann, C. W. (1994) *Int. J. Cancer 57*, 684−690.
4. Ebralidze, A., Tulchinsky, E., Grigorian, M., Afanasyeva, A., Senin, V., Revazova, E., and Lukanidin, E. (1989) *Genes Dev. 3*, 1086−1093.
5. Grigorian, M., Tulchinsky, E., Burrone, O., Tarabykina, S., Georgiev, G., and Lukanidin, E. (1994) *Electrophoresis 15*, 463−468.
6. Grigorian, M. S., Tulchinsky, E. M., Zain, S., Ebralidze, A. K., Kramerov, D. A., Kriajevska, M. V., Georgiev, G. P., and Lukanidin, E. M. (1993) *Gene 135*, 229−238.
7. Grigorian, M., Ambartsumian, N., Lykkesfeldt, A. E., Bastholm, L., Elling, F., Georgiev, G., and Lukanidin, E. (1996) *Int. J. Cancer 67*, 831−841.
8. Davies, B. R., Davies, M. P., Gibbs, F. E., Barraclough, R., and Rudland, P. S. (1993) *Oncogene 8*, 999−1008.
9. Davies, B. R., Barraclough, R., and Rudland, P. S. (1994) *Cancer Res. 54*, 2785−2793.
10. Davies, M. P., Harris, S., Rudland, P. S., and Barraclough, R. (1996) *Biochem. Soc. Trans. 24*, 356S.
11. Ambartsumian, N. S., Grigorian, M. S., Larsen, I. F., Karlstrom, O., Sidenius, N., Rygaard, J., Georgiev, G., and Lukanidin, E. (1996) *Oncogene 13*, 1621−1630.
12. Maelandsmo, G. M., Hovig, E., Skrede, M., Engebraaten, O., Florenes, V. A., Myklebost, O., Grigorian, M., Lukanidin, E., Scanlon, K. J., and Fodstad, O. (1996) *Cancer Res. 56*, 5490−5498.
13. Takenaga, K., Nakamura, Y., and Sakiyama, S. (1997) *Oncogene 14*, 331−337.
14. Ford, H. L., and Zain, S. B. (1995) *Oncogene 10*, 1597−1605.
15. Ford, H. L., Salim, M. M., Chakravarty, R., Aluiddin, V., and Zain, S. B. (1995) *Oncogene 11*, 2067−2075.
16. Kriajevska, M. V., Cardenas, M. N., Grigorian, M. S., Ambartsumian, N. S., Georgiev, G. P., and Lukanidin, E. M. (1994) *J. Biol. Chem. 269*, 19679−19682.
17. Kriajevska, M., Bronstein, I. B., Scott, D. J., Tarabykina, S., Fischer-Larsen, M., Issinger, O., and Lukanidin, E. (2000) *Biochim. Biophys. Acta 1498*, 252−263.
18. Donato, R. (1999) *Biochim. Biophys. Acta 1450*, 191−231.
19. Kilby, P. M., Van Eldik, L. J., and Roberts, G. C. (1997) *Protein Sci. 6*, 2494−2503.
20. Rustandi, R. R., Baldisseri, D. M., and Weber, D. J. (2000) *Nat. Struct. Biol. 7*, 570−574.
21. Deloulme, J. C., Assard, N., Mbele, G. O., Mangin, C., Kuwano, R., and Baudier, J. (2000) *J. Biol. Chem. 275*, 35302−35310.
22. Rety, S., Sopkova, J., Renouard, M., Osterloh, D., Gerke, V., Tabaries, S., Russo-Marie, F., and Lewit-Bentley, A. (1999) *Nat. Struct. Biol. 6*, 89−95.
23. Osterloh, D., Ivanenkov, V. V., and Gerke, V. (1998) *Cell Calcium 24*, 137−151.
24. Alexandrov, A., Dutta, K., and Pascal, S. M. (2001) *BioTechniques 30*, 1194−1198.
25. Dutta, K., Cox, C., Alexandrov, A., Huang, H., Zain, S., Basavappa, R., and Pascal, S. M. (2002) *J. Biomol. NMR* (in press).
26. Kay, L. E., Keifer, P., and Saarinen, T. (1992) *J. Am. Chem. Soc. 114*, 10663−10665.
27. Delaglio, F., Grzesiek, S., Vuister, G. W., Zhu, G., Pfeifer, J., and Bax, A. (1995) *J. Biomol. NMR 6*, 277−293.
28. Johnson, B. A., and Blevins, R. A. (1994) *J. Biomol. NMR 4*, 603−614.
29. Biekofsky, R. R., Martin, S. R., Browne, J. P., Bayley, P. M., and Feeney, J. (1998) *Biochemistry 37*, 7617−7629.
30. Forsen, S., Drakenberg, T., and Wennerstrom, H. (1987) *Q. Rev. Biophys. 19*, 83−114.
31. Akke, M., Forsen, S., and Chazin, W. J. (1991) *J. Mol. Biol. 220*, 173−189.
32. Dukhanina, E. A., Dukhanin, A. S., Lomonosov, M. Y., Lukanidin, E. M., and Georgiev, G. P. (1997) *FEBS Lett. 410*, 403−406.
33. Wishart, D. S., and Sykes, B. D. (1994) *J. Biomol. NMR 4*, 171−180.
34. Drohat, A. C., Baldisseri, D. M., Rustandi, R. R., and Weber, D. J. (1998) *Biochemistry 37*, 2729−2740.
35. Drohat, A. C., Tjandra, N., Baldisseri, D. M., and Weber, D. J. (1999) *Protein Sci. 8*, 800−809.
36. Skelton, N. J., Kordel, J., and Chazin, W. J. (1995) *J. Mol. Biol. 249*, 441−462.
37. Kordel, J., Pearlman, D. A., and Chazin, W. J. (1997) *J. Biomol. NMR 10*, 231−243.
38. Moroz, O. V., Antson, A. A., Murshudov, G. N., Maitland, N. J., Dodson, G. G., Wilson, K. S., Skibshoj, I., Lukanidin, E. M., and Bronstein, I. B. (2001) *Acta Crystallogr. D57*, 20−29.
39. Rety, S., Osterloh, D., Arie, J. P., Tabaries, S., Seeman, J., Russo-Marie, F., Gerke, V., and Lewit-Bentley, A. (2000) *Struct. Folding Des. 8*, 175−184.
40. Ishikawa, K., Nakagawa, A., Tanaka, I., Suzuki, M., and Nishihira, J. (2000) *Acta Crystallogr. D56*, 559−566.
41. Brodersen, D. E., Etzerodt, M., Madsen, P., Celis, J. E., Thogersen, H. C., Nyborg, J., and Kjeldgaard, M. (1998) *Structure 6*, 477−489.
42. Brodersen, D. E., Nyborg, J., and Kjeldgaard, M. (1999) *Biochemistry 38*, 1695−1704.
43. Guex, N., and Peitsch, M. C. (1997) *Electrophoresis 18*, 2714−2723.

BI012061V